

Scrambling is Necessary but Not Sufficient for Chaos

Neil Dowling,^{1,*} Pavel Kos,^{2,3} and Kavan Modi^{1,4}

¹*School of Physics & Astronomy, Monash University, Clayton, VIC 3800, Australia*

²*Max-Planck-Institut für Quantenoptik, Hans-Kopfermann-Str. 1, 85748 Garching*

³*Munich Center for Quantum Science and Technology (MCQST), Schellingstr. 4, 80799 München, Germany*

⁴*Centre for Quantum Technology, Transport for New South Wales, Sydney, NSW 2000, Australia*

(Dated: April 18, 2023)

We show that out-of-time-order correlators (OTOCs) constitute a probe for Local-Operator Entanglement (LOE). There is strong evidence that a volumetric growth of LOE is a faithful dynamical signature of quantum chaos, while OTOC decay corresponds to operator scrambling, often conflated with chaos. We show that rapid OTOC decay is a necessary but not sufficient condition for linear (chaotic) growth of the LOE entropy. We analytically support our results through wide classes of local-circuit models of many-body dynamics, including both integrable and non-integrable dual-unitary circuits. We show sufficient conditions under which local dynamics leads to an equivalence of scrambling and chaos.

Introduction.— In recent years, a wide plethora of apparently inequivalent notions of quantum chaos have sprung up. A popular candidate is the out-of-time-ordered correlator (OTOC), which measures a notion of scrambling in many-body systems [1–5]. In this Letter, we will give a novel interpretation for the OTOC by showing that it serves as a particular probe to the Local-Operator Entanglement (LOE), a well justified measure of dynamical complexity and quantum chaos [6, 7]. In doing so, we will uncover simple cases where a dynamics is scrambling and so leads to an exponential OTOC scaling, yet is not chaotic as demonstrated by linear LOE entropy growth. Along the way, we derive exact analytical results for a class of many-body local circuits [8, 9]. Our results show a clear distinction between scrambling and chaos, namely, scrambling is necessary but not sufficient for quantum chaos.

The LOE is a measure of the complexity scaling of a Heisenberg operator $V_t := e^{iHt}(V_B \otimes \mathbb{1}_{\bar{B}})e^{-iHt}$ corresponding to an initially local operator V [6]. V acts on a space \mathcal{H}_B , whereas V_t acts on the full system $\mathcal{H}_S = \mathcal{H}_B \otimes \mathcal{H}_{\bar{B}}$. Above, H is a many-body Hamiltonian. This is directly proportional to the classical simulability of an evolution [6, 10], with its scaling with time indicative of the integrability of the dynamics [7, 11–17]. Specifically, the LOE is the entanglement of the Choi state of an initially local, unitary and traceless Heisenberg operator V_t ,

$$|V_t\rangle := (V_t \otimes \mathbb{1})|\phi^+\rangle, \quad (1)$$

where $|\phi^+\rangle$ is the maximally entangled state over a doubled system. As this is a pure quantum state, we can

analyze its static quantum mechanical properties such as its entanglement (LOE).

LOE is an attractive candidate for an operational and complete notion of quantum chaos, given that: (i) volume-law (linearly growing) LOE implies both that a local quantum circuit representation of the unitary needs to be a maximal depth and that it is difficult to simulate classically (consistent with the result of Ref. [18]), (ii) a wide range of studies into physical models support that volume-law LOE is a necessary and sufficient indicator of chaos, with an at-most logarithmic growth for (interacting) integrable systems [7, 11, 13–17], and (iii) it can be understood as a sensitivity to perturbation, analogous to classical chaos [19]. Note that the simple growth of entanglement of *states* in a quantum many-body system is not a signature of chaos, with e.g. Clifford circuits and non-interacting models generally exhibiting a linear growth [20, 21]. Further, the LOE should not be confused with the related quantity of the ‘operator entanglement’, which is the entanglement of the Choi state of the full, global unitary evolution operator [22, 23]. This quantity does not have the same connection to chaos as the LOE, generally scaling linearly with t irrespective of integrability [13], unless the Hamiltonian is in a localized phase [24].

The OTOC, on the other hand, indicates a kind of operator scrambling, and is defined as a four-point correlator with atypical time ordering [1–5],

$$F(W, V_t) = \frac{1}{d} \text{tr}[W^\dagger V_t^\dagger W V_t], \quad (2)$$

where we take this expectation value to be computed over the maximally mixed state $\rho_\infty = \mathbb{1}/d$. We take V and W to be local unitaries, in which case it is easy to prove that the OTOC is directly proportional to the square

* neil.dowling@monash.edu

commutator of the Heisenberg operators,

$$\text{Re}[F(W, V_t)] = 1 - \frac{1}{2} \langle [W, V_t]^2 \rangle. \quad (3)$$

That is, the OTOC quantifies how much V_t anti-commutes with W as a function of time. The appeal for OTOC stems from a semiclassical argument connecting the last equation to classical Poisson brackets, which are directly related to the Lyapunov exponents of a classical process.

Yet, it remains unclear why should this measure chaos? In fact, there is controversy in when the OTOC detects chaos in a wide range of quantum systems without a classical analogue [25–28] or even with [29, 30]. In this Letter we shed light on this confusion, showing how the OTOC probes dynamical chaos, including how it can fail in this purpose and specifying sufficient conditions when scrambling is equivalent to chaos.

OTOC in Terms of Local Operator Choi State.— We consider the OTOC with unitary operators V and W , which wlog are taken to be traceless - this is the only part of a general unitary V that scales with time; see App. A. We take W to be acting on some potentially large subspace \mathcal{H}_A and V on a local space \mathcal{H}_B , with complement spaces defined such that the whole isolated system is $\mathcal{H}_S = \mathcal{H}_A \otimes \mathcal{H}_{\bar{A}} = \mathcal{H}_B \otimes \mathcal{H}_{\bar{B}}$. These spaces are most clearly expressed via the graphical representation of the the OTOC $F(W, V_t)$ (Eq. (2)), equal to

$$\frac{1}{d} \text{tr} \left[\begin{array}{c} \text{A} \\ \text{A}' \\ \text{A}'' \end{array} \left[\begin{array}{c} \text{U}_t^\dagger \\ \text{V} \\ \text{U}_t \end{array} \right] \left[\begin{array}{c} \text{W} \\ \text{U}_t^\dagger \\ \text{V}^\dagger \\ \text{U}_t \end{array} \right] \left[\begin{array}{c} \text{W}^\dagger \\ \text{B} \end{array} \right] \right].$$

We will also use a bracket-prime notation to indicate a doubled space. In particular, a prime label A' represents a copy of the space A , while bracketed primes represent a combined double space, $\mathcal{H}_{B^{(0)}} := \mathcal{H}_B \otimes \mathcal{H}_{B'}$. For clarity, we rewrite the definition of the Choi state $|V_t\rangle$ (Eq. (1)),

$$|V_t\rangle := \frac{1}{d} \begin{array}{c} \text{B}' \\ \text{B} \\ \text{B}'' \end{array} \left[\begin{array}{c} \text{U}_t \\ \text{U}_t^* \end{array} \right] \begin{array}{c} \text{B} \\ \text{B}' \end{array} = \begin{array}{c} \text{B}^{(0)} \\ \text{B}^{(0)} \end{array} \left[\begin{array}{c} \text{V}_t \end{array} \right]. \quad (4)$$

In this setup, V_t can be interpreted as the time evolved local Heisenberg operator we are interested in, and W as the *probe* to the entanglement of the Choi state of this operator, Eq. (1). We see the first hint of this relation, in the following observation.

Observation 1. *The OTOC can be expressed in terms of the expectation value of a local unitary, $\mathcal{W} := W \otimes W^*$, with respect to the Choi state of a time evolved Heisenberg operator, $|V_t\rangle$,*

$$F(W, V_t) = \langle V_t | (\mathbb{1}_{\bar{A}^{(0)}} \otimes \mathcal{W}) | V_t \rangle. \quad (5)$$

The proof for this, and all following results, can be found in the Appendix.

Examining the relation Eq. (5), if $|V_t\rangle$ is maximally entangled in the splitting $A^{(0)} : \bar{A}^{(0)}$, then the OTOC is equal to zero. Recalling that any maximally entangled state ψ corresponds to the Choi state of a unitary matrix \mathcal{U}_ψ , one can prove this from Eq. (5) using standard graphical notation:

$$F(W, V_t) = \frac{1}{d} \begin{array}{c} \text{U}_\psi^\dagger \\ \text{W} \\ \text{U}_\psi \end{array} = |\text{tr}[W]|^2 = 0. \quad (6)$$

For example, a global Haar random time evolution, $U_t \in \mathbb{H}$, with a large total dimension d , will approximately give a maximally entangled $|V_t\rangle$ on average. We show this in App. C.

Alternatively, if $|V_t\rangle$ is not maximally entangled, $F(W, V_t)$ will generally be non-zero, suggesting that this quantity constitutes a probe of the LOE of V_t , through an operator W . We will now quantify this relationship in the following, showing the necessity of OTOC decay for chaotic LOE behavior.

Chaos Implies Scrambling.— To investigate the general behavior of the OTOC, we will now compute its average value when a random traceless operator W is sampled, and show that this sampling is typical. To uniformly sample a random matrix with the traceless property, a natural choice is to choose any traceless unitary W and then apply a Haar random unitary channel to it, $W_R = R^\dagger W R$ where $R \in \mathbb{H}$. \mathbb{H} refers to the Haar ensemble: the unique, unitarily invariant measure on the space of unitary matrices $\mathbb{U}(d)$. We define the averaged OTOC with respect to this traceless probe,

$$G(V_t) := \frac{1}{d} \int_{\mathbb{H}} dR \text{tr}[W_R^\dagger V_t^\dagger W_R V_t]. \quad (7)$$

We stress that we are not averaging over the dynamics, and allow the time-evolution operator U_t to be completely arbitrary. Hinting at the relation of the OTOC to entanglement, our results will be framed in terms of $\nu_A(t)$, the (normalized) reduced density matrix of the Choi state $|V_t\rangle$ on (the doubled space) $\mathcal{H}_{A^{(0)}} = \mathcal{H}_A \otimes \mathcal{H}_{A'}$,

$$\nu_A(t) := \text{tr}_{\bar{A}^{(0)}}[|V_t\rangle\langle V_t|]. \quad (8)$$

We can then use standard techniques adapted from the Weingarten Calculus to arrive at our first main result.

Theorem 2. *The averaged OTOC over Haar random, traceless unitaries W (as in Eq. (7)) is equal to*

$$G(V_t) = \frac{1}{d_A^2 - 1} \left(d_A^2 \langle \phi^+ | \nu_A(t) | \phi^+ \rangle - 1 \right), \quad (9)$$

where $|\phi^+\rangle$ is the maximally entangled state across the doubled system $\mathcal{H}_{S^{(0)}}$.

Notice that the first term is proportional to the fidelity between $\nu_A(t)$ and the identity matrix Choi state $|\phi^+\rangle\langle\phi^+|$. In words, this theorem states that the average OTOC is *proportional to the distance between the actual reduced state of $|V_t\rangle$ on $\mathcal{H}_{A^{(0)}}$ and the state of the identity channel*. Interestingly, considering V_t as a unitary channel, this fidelity is exactly equal to the entanglement fidelity of the reduced channel on \mathcal{H}_A , which in turn is proportional to the (efficiently computable) average gate fidelity [31].

Remarkably, the following concentration of measure bound shows that a random $F(W, V_t)$ rarely varies from the average $G(V_t)$. This is important as we work concerns this OTOC average $G(V_t)$ in rest of the paper, and we can be assured that the average case is representative of the typical one.

Proposition 3. *The probability that the OTOC $F(W_R, V_t)$ for some Haar random, traceless unitary W_R varies from the average $G(V_t)$ by more than some $\epsilon > 0$, satisfies*

$$\Pr_{R \sim \mathbb{H}} \{|F(W_R, V_t) - G(V_t)| \geq \epsilon\} \leq \exp\left(-\frac{d_A^2 \epsilon^2}{64}\right). \quad (10)$$

This means that if one chooses the traceless ‘probing’ unitary W in the OTOC $F(W, V_t)$ to be Haar random and acting on a relatively large subspace \mathcal{H}_A , then it is exponentially likely to approximately satisfy Theorem 2 and all following results where $G(V_t)$ appears. Even if \mathcal{H}_A is composed of only $\mathcal{O}(10^1)$ qubits, the right hand side of Eq. (10) gives a confidence of $\mathcal{O}(1/e^4) \sim 0.0183$ within an error of $\epsilon \sim \mathcal{O}(2^{-6}) \sim 0.0156$.

Ref. [23] reports similar results to Thm 2 and Prop. 3. However, there the Haar average is taken for the ‘bipartite OTOC’ over *both* V and W , which are taken to have support that is disjoint, but jointly covers the whole system. Our results are distinct, and far less restrictive, in allowing the operators to have arbitrary locality, averaging over only one of the unitaries, and most importantly connecting this to the LOE (chaos).

We will now consider a number of example dynamics to pick apart Theorem 2. First, if V_t has no support on \mathcal{H}_A , then $\nu_A(t) = |\phi^+\rangle\langle\phi^+|$ and so as expected $G(V_t) = 1$. Typical examples are locally interacting systems at short times, whereby one operator lies outside the lightcone of the other. Next, consider a dynamics consisting of a circuit of swaps $U_t \in \mathbb{S}$. Then, if the operator V is swapped onto a site within the space \mathcal{H}_A , the OTOC takes a minimum value,

$$G(V_t)|_{U_t \in \mathbb{S}} = \begin{cases} \frac{-1}{d_A^2 - 1}, & \text{if } V_t \in \mathcal{B}(\mathcal{H}_A) \\ 1, & \text{otherwise.} \end{cases} \quad (11)$$

given that V is taken to be traceless. Similarly, one would (approximately) get this result for $\nu_A(t)$ being (close to)

any pure state which is orthogonal to $|\phi^+\rangle\langle\phi^+|$. This is an example of a kind of scrambling without chaos: a minimal OTOC is achieved for a clearly integrable dynamics. Such a dynamics is not a unique example of scrambling without chaos. In fact, it is a simple example of a wide class of local circuit models, which we will analyze later in Results 6-8. Finally, we saw earlier in Eq. (6) that a maximally entangled $|V_t\rangle$ leads to a small OTOC. This begs the question of what the OTOC tells us if $|V_t\rangle$ is partially entangled? Can we further understand this OTOC average as a quantitative probe to the time-scaling of the LOE?

We now give two bounds, in terms of two different measures of entanglement, supporting the proposition that fast OTOC decay necessarily leads to chaotic LOE growth.

Theorem 4. (Scrambling is Necessary for Chaos) *The OTOC, averaged over traceless unitary operators W , is bounded by the entanglement of the time-evolved local operator V_t in the bipartition $(A^{(t)} : \bar{A}^{(t)})$:*

A. *For geometric measure of entanglement, $E_G(|\phi\rangle) := 1 - \max_{|\psi_{A^{(t)}}\psi_{\bar{A}^{(t)}}\rangle} |\langle\psi_{A^{(t)}}\psi_{\bar{A}^{(t)}}|\phi\rangle|^2$, where the maximum is over all product states $|\psi_{A^{(t)}}\psi_{\bar{A}^{(t)}}\rangle$, $G(V_t)$ satisfies*

$$G(V_t) \leq 1 - \frac{d_A^2}{d_A^2 - 1} E_G(|V_t\rangle). \quad (12)$$

B. *For the 2-Rényni entropy $S^{(2)}(\nu) := -\log(\text{tr}[\nu^2])$, $G(V_t)$ satisfies*

$$G(V_t) \leq \frac{1}{d_A^2 - 1} \left(d_A^2 e^{-\frac{1}{2} S^{(2)}(\nu_A(t))} - 1 \right). \quad (13)$$

Note that we only used the inequality $\mathcal{D}(\nu_A(t), |\phi^+\rangle\langle\phi^+|) \leq \max_{|\psi\rangle} (\mathcal{D}(\nu_A(t), |\psi\rangle\langle\psi|))$ for some distance metric \mathcal{D} , to arrive at Eq. (12). Therefore it is likely relatively tight for a generic evolution, where V_t does not recollapse into a local, pure unitary channel. Indeed, from numerics we notice that Eq. (12) seems to be tighter than Eq. (13). However, in general geometric measures are not practically accessible due to the required optimization over all separable states. On the other hand, the Rényi 2-entropy is. The bound (13) is therefore one of our main results, and will be investigated in the remainder of this work.

The LOE entropy grows at fastest linearly, with strong evidence that this maximal scaling is saturated if and only if the dynamics are chaotic [14, 16], compared to logarithmic growth for integrable dynamics [7, 11–13, 15, 17]. Therefore, Eq. (13) gives us a bound on scrambling, with the OTOC decaying at fastest exponentially, governed by the rate of growth of the LOE entropy,

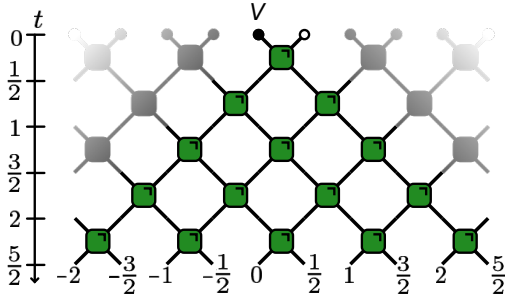


FIG. 1. Brickwork circuit models of dynamics consists of repeated 2-site unitary superoperators on a one dimensional lattice. Time goes from top to bottom, and the lightcone for a single-site operator is shown in green. We set wlog the position of the initial local operator V to be $y = 0$.

$$G(V_t) \lesssim \begin{cases} B \exp(-\alpha t), & \text{if } U_t \text{ chaotic,} \\ C t^{-\alpha}, & \text{if } U_t \text{ regular.} \end{cases} \quad (14)$$

This should not be compared to the bound on certain OTOCs from Refs. [3, 32]. There they *lower-bound* a thermally regulated OTOC within a certain time regime with an exponential function with positive Lyapunov exponent for fast-scrambling systems, under a range of assumptions and approximations. The strength of Theorem 4 is that it is an analytic argument relying on essentially no assumptions, with the scaling (14) determined by a range of previous heuristics [7, 11–17].

Theorem 4 therefore states that fast decay of the OTOC is necessary for chaos. However, the counter argument is not necessarily true, i.e. the bounds in Eq. (14) are not necessarily tight. We will now examine our results through classes of local circuit models, to uncover: (i) When Eq. (13) is saturated, and (ii) When the OTOC decays fast for slowly decaying LOE; i.e. scrambling without chaos.

Application to Local Circuit Models.— We will now consider examples of local circuit models of dynamics, called ‘brickwork’ circuits [21, 33–37], whereby at each discrete time step two-body unitary gates are applied to next-neighbor sites on a lattice (see Fig. 1),

$$U : \mathcal{H}_{i_1} \otimes \mathcal{H}_{i_2} \rightarrow \mathcal{H}_{o_1} \otimes \mathcal{H}_{o_2}. \quad (15)$$

It is necessary to introduce some notation to succinctly present our results. We take the initial operator V to have support on a single site which we specify wlog to be at $y = 0$, where both the sites and time steps are labeled with half integers as in Fig. 1. Then the disjoint spaces \mathcal{H}_A and $\mathcal{H}_{\bar{A}}$ are labeled by the list of integers of the spins they contain, ℓ_A and $\ell_{\bar{A}}$ respectively. The following results will cover two exclusive cases: when the left light cone edge is in \mathcal{H}_A ($t \in \ell_A$) or when the right light cone is in \mathcal{H}_A ($t \in \ell_{\bar{A}}$), where we denote by a the edge of region

$\mathcal{H}_{A^{(0)}}$ within the lightcone. Finally, we define $x_{\pm} := t \pm a$ as the ‘light cone coordinates’ (see Fig. 2).

In completely general brickwork unitary circuits, both the OTOC and the LOE entropy can be expressed in terms of the same spacetime transfer matrix $G(V_t)^2 \sim (\mathcal{T}_{x_+}[U])^{x_-} \sim S^{(2)}(\nu_A(t))$. While we do not define \mathcal{T} explicitly here (see App. G), this leads to our first result on local circuit OTOC behavior.^[38]

Observation 5. *When the term $-\frac{1}{d_A^2-1}$ from Eq. (9) can be neglected, both sides of the inequality Eq. (13) have generically the same leading order scaling for large x_- , but constant x_+ .*

Further supporting this result, numerical examples of Haar random unitary bricks show similar scaling for both sides of Eq. (13). We will now delve into a specific model in order to uncover an analytic example showing that scrambling is distinct from chaos.

Consider the Floquet interacting XXZ model on qubits, consisting of a brickwork dynamics (see Fig. 1) with two-site unitary

$$U_{\text{XXZ}} = \exp \left[-i \left(\frac{\pi}{4} \sigma_x \otimes \sigma_x + \frac{\pi}{4} \sigma_y \otimes \sigma_y + J \sigma_z \otimes \sigma_z \right) \right]. \quad (16)$$

where J is a free parameter. We have set the parameter in front of $\sigma_x \otimes \sigma_x$ and $\sigma_y \otimes \sigma_y$ to $\pi/4$ to impose dual-unitarity [9, 39, 40], which we later discuss. Moreover, we additionally specify that $J \neq \pi/4$, as $J = \pi/4$ yields the SWAP circuit as in Eq. (11). This dynamics is not chaotic. In particular, the LOE scales logarithmically with time [12, 17], characteristic of interacting integrable models. However, we will see that the OTOC decays exponentially for all times (or is constantly minimal), indicative of strong scrambling.

Theorem 6. (Scrambling without Chaos) *The Floquet dual-unitary XXZ model (16) produces an exponentially decaying OTOC. Concretely, for a single site operator V , Eq. (18) reduces to*

$$G(V_t)|_{\text{XXZ}} = \begin{cases} \frac{-1}{d_A^2-1}, & \text{if } t \in \ell_A \\ \beta e^{-\alpha(x_-)} + (1-\beta), & \text{if } t \in \ell_{\bar{A}}. \end{cases} \quad (17)$$

with positive constants α and β reported in Eq. (H6). For any V orthogonal to σ_z , the constants are such that $G(V_t)$ decays to a minimal (negative) value.

The fact that the OTOC exhibits (maximal) exponential decay for this clearly integrable model is stark evidence of the distinction between scrambling and chaos. This lays bare the main thesis of this Letter: while the OTOC will always bear witness to chaos, there exists a wide variety of dynamics that are scrambling but not chaotic. In other words, *the decay of the OTOC is necessary but not sufficient for chaos.*

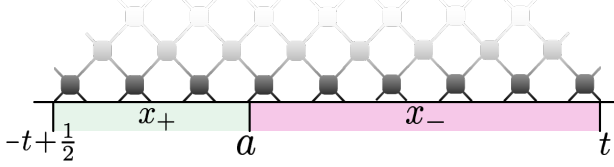


FIG. 2. Schematic of the labeling conventions used in our results for brickwork circuits. x_- describes the size of the region $\mathcal{H}_{A^{(t)}}$ ($\mathcal{H}_{\bar{A}^{(t)}}$) when $t \in \ell_A$ ($t \in \ell_{\bar{A}}$).

The example dynamics (16) is in fact a particular example of a class of locally interacting models that are considered to yield maximally spreading dynamics [9, 41, 42]. Using Eq. (9), we can actually compute the average OTOC for this entire class of many-body dynamics that satisfy the dual unitary property, which we call \mathbb{D} . These are local circuits where each component is unitary in both the space and time direction, such that one can analytically compute a range of relevant quantities in many-body systems evolving under these dynamics. Far beyond the trivial swap circuit \mathbb{S} as in Eq. (11), these models include for example the (chaotic) self-dual kicked Ising model [8, 43, 44] and the (integrable) Floquet Heisenberg XXZ model [39, 40], as in Eq. (16). Dual unitarity is a highly general condition on two-body gates, setting only two out of the 16 free parameters of the 2-qubit unitary group [9].

We define a necessary object which is well-studied in dual unitary literature [9]. In terms of the (doubled) local, bipartite Hilbert spaces as in Eq. (15), we define the CPTP maps $\mathcal{M}_+ := \langle \mathbb{1}_{i_1^{(t)}} U^* \otimes U | \mathbb{1}_{o_2^{(t)}} \rangle$ and $\mathcal{M}_- := \langle \mathbb{1}_{i_2^{(t)}} U^* \otimes U | \mathbb{1}_{o_1^{(t)}} \rangle$. These local maps govern the decay of 2-point correlations in \mathbb{D} [9]. Remarkably, we can compute the OTOC average for this entire class exactly, where it either takes a uniform, minimal value, or otherwise always generically decays exponentially.

Theorem 7. (OTOC in Dual Unitary Circuits) *For evolution according to dual unitary circuits \mathbb{D} , the average OTOC is exactly*

$$G(V_t)|_{\mathbb{D}} = \begin{cases} -\frac{1}{d_A^2 - 1}, & t \in \ell_A \\ \frac{1}{d_A^2 - 1} (d_A^2 \langle V | \mathcal{M}_+^{x_+} \mathcal{M}_-^{x_-} | V \rangle - 1), & t \in \ell_{\bar{A}}. \end{cases} \quad (18)$$

We stress that our result for $G(t)$ in Eq. (18) relies *only* on the dual unitarity property, both in the chaotic and non-chaotic cases. Note that the present work is not unique in considering OTOCs in dual unitary circuits. In Ref. [41], OTOCs are computed in the ‘infinite lightcone’ limit for the subset of completely chaotic dual unitary circuits, while in Ref. [45] average OTOCs are computed for circuits consisting of randomly sampled 1-site parts of dual unitary qubit gates. Neither of these references

compute the OTOC averaged over one of the operators W , for arbitrary t . In addition, in our case the support of W can be arbitrary large, in contrast to the single site operators considered in these works.

We can further specify the dual unitary dynamics to be ‘completely chaotic’ [16] (‘maximally chaotic’ in Ref. [41]), defined by the property that the eigenvectors with eigenvalue one of the transfer matrix discussed around Observation 5 are limited to a minimal set (see App. G). This property generically holds, but is violated if there are additional symmetries (e.g. kicked Ising model) or additional local conservation laws (e.g. trotterized XXZ model). This property leads to a precise equivalence between the LOE and OTOC.

Corollary 8. *For x_- kept fixed, Eq. (18) can be expressed using the known inequalities of Rényi-2 entropy of LOE (see App. G) as*

$$G(V_t)|_{U_t \in \mathbb{D}} \leq \exp \left[\lim_{x_- \rightarrow \infty} \frac{-1}{2} S^{(2)}(\nu_A(t)) \right], \quad (19)$$

where equality holds exactly for completely chaotic dual unitary circuits for $|\lambda| \geq d^{-1/2}$, and also taking x_+ to be large. Here, $|\lambda|$ is the largest non-trivial eigenvalue of \mathcal{M}_- [16].

Notice here that Eq. (19) is exactly equivalent to Eq. (13) for $d_A \gg 1$. That is, asymptotically the average OTOC is proportional to LOE in completely chaotic dual unitary circuits with $|\lambda| \geq d^{-1/2}$. This provides an important new insight into the completely chaotic assumption: for dual unitary circuits it is equivalent to demanding equality in (13). It would be interesting to study when this inequality (13) is saturated for non dual-unitary circuits, which we discuss in our concluding remarks.

Conclusions and Discussion.— In this Letter, we have demonstrated that the Out-of-Time-Ordered Correlator (OTOC) generally functions as a probe of the Local Operator Entanglement (LOE) of the time-evolving operator V_t (Results 1- 4). This means that formally, scrambling is strictly necessary for chaos. To explore this relationship, we examined the OTOC for the class of dual unitary local circuits. We showed an explicit example of an integrable dynamics where the OTOC exponentially decays for all times, representing a maximal scrambling without chaos (Theorem 6). Finally, we also determined generic conditions that defines when LOE scaling is precisely equivalent to OTOC scaling in dual unitary circuits (Theorem 7).

In this work, the (ultra-)local unitary operator V was left unspecified, but its exact choice may influence computations (cf. Thm 6). Often, it is argued that typically the particular choice of operator V should not matter (for OTOC), therefor V is averaged over [46, 47]. One can

take a more subtle approach and define a density operator that encodes all possible OTOCs or local Heisenberg operators, which is therefore independent of the choice of local operator [19, 48]. We extend our main results to this operator-free setting in App. I.

We saw in Theorem 7 that in local circuits which satisfy the (distinctly) dual unitary property of being completely chaotic, in some cases scrambling equals chaos. It would be interesting to determine the class of models which saturate the bound (13) in general evolution which does not satisfy the dual unitary property. We speculate that (13) may hold the key to characterizing a class of completely chaotic evolution in this general case.

Finally, there is some motivation in recent literature that the usual (4-point) OTOC which we consider here does not probe a sufficiently fine structure of chaos and randomness [18, 46]. Instead, a higher point OTOC generalization is sometimes considered, called the $2k$ -OTOC. There is a clear generalization of the present results connecting such higher OTOCs to a novel gener-

alization of LOE, but we leave this to a future detailed investigation.

ACKNOWLEDGMENTS

PK thanks Georgios Styliaris for fruitful discussions. We acknowledge funding from the DAAD Australia-Germany Joint Research Cooperation Scheme through the project 57445566. ND is supported by an Australian Government Research Training Program Scholarship and the Monash Graduate Excellence Scholarship. PK acknowledges financial support from the Alexander von Humboldt Foundation. KM acknowledges support from the Australian Research Council Future Fellowship FT160100073, Discovery Projects DP210100597 and DP220101793, and the International Quantum U Tech Accelerator award by the US Air Force Research Laboratory.

-
- [1] A. Kitaev, 2015 breakthrough prize fundamental physics symposium, URL: <https://breakthroughprize.org/Laureates/1/L3> (2014).
 - [2] S. H. Shenker and D. Stanford, Black holes and the butterfly effect, *Journal of High Energy Physics* **2014**, 67 (2014).
 - [3] J. Maldacena, S. H. Shenker, and D. Stanford, A bound on chaos, *Journal of High Energy Physics* **2016**, 106 (2016).
 - [4] B. Swingle, G. Bentsen, M. Schleier-Smith, and P. Hayden, Measuring the scrambling of quantum information, *Phys. Rev. A* **94**, 040302 (2016).
 - [5] D. A. Roberts and B. Swingle, Lieb-robinson bound and the butterfly effect in quantum field theories, *Phys. Rev. Lett.* **117**, 091602 (2016).
 - [6] T. Prosen and M. Znidarič, Is the efficiency of classical simulations of quantum dynamics related to integrability?, *Phys. Rev. E* **75**, 015202(R) (2007).
 - [7] T. Prosen and I. Pižorn, Operator space entanglement entropy in a transverse ising chain, *Phys. Rev. A* **76**, 032316 (2007).
 - [8] M. Akila, D. Waltner, B. Gutkin, and T. Guhr, Particle-time duality in the kicked ising spin chain, *Journal of Physics A: Mathematical and Theoretical* **49**, 375101 (2016).
 - [9] B. Bertini, P. Kos, and T. Prosen, Exact correlation functions for dual-unitary lattice models in 1 + 1 dimensions, *Phys. Rev. Lett.* **123**, 210601 (2019).
 - [10] M. J. Hartmann, J. Prior, S. R. Clark, and M. B. Plenio, Density matrix renormalization group in the heisenberg picture, *Phys. Rev. Lett.* **102**, 057202 (2009).
 - [11] I. Pižorn and T. Prosen, Operator space entanglement entropy in xy spin chains, *Phys. Rev. B* **79**, 184416 (2009).
 - [12] D. Muth, R. G. Unanyan, and M. Fleischhauer, Dynamical simulation of integrable and nonintegrable models in the heisenberg picture, *Phys. Rev. Lett.* **106**, 077202 (2011).
 - [13] J. Dubail, Entanglement scaling of operators: a conformal field theory approach, with a glimpse of simulability of long-time dynamics in 1...1d, *Journal of Physics A: Mathematical and Theoretical* **50**, 234001 (2017).
 - [14] C. Jonay, D. A. Huse, and A. Nahum, Coarse-grained dynamics of operator and state entanglement (2018), [arXiv:1803.00089 \[cond-mat.stat-mech\]](https://arxiv.org/abs/1803.00089).
 - [15] V. Alba, J. Dubail, and M. Medenjak, Operator entanglement in interacting integrable quantum systems: The case of the rule 54 chain, *Phys. Rev. Lett.* **122**, 250603 (2019).
 - [16] B. Bertini, P. Kos, and T. Prosen, Operator Entanglement in Local Quantum Circuits I: Chaotic Dual-Unitary Circuits, *SciPost Phys.* **8**, 067 (2020).
 - [17] V. Alba, Diffusion and operator entanglement spreading, *Phys. Rev. B* **104**, 094410 (2021).
 - [18] L. Leone, S. F. E. Oliviero, Y. Zhou, and A. Hamma, Quantum Chaos is Quantum, *Quantum* **5**, 453 (2021).
 - [19] N. Dowling and K. Modi, Quantum Chaos = Volume-Law Spatiotemporal Entanglement (2022), [arXiv:2210.14926 \[quant-ph\]](https://arxiv.org/abs/2210.14926).
 - [20] M. Fagotti and P. Calabrese, Evolution of entanglement entropy following a quantum quench: Analytic results for the xy chain in a transverse magnetic field, *Phys. Rev. A* **78**, 010306 (2008).
 - [21] C. W. von Keyserlingk, T. Rakovszky, F. Pollmann, and S. L. Sondhi, Operator hydrodynamics, otocs, and entanglement growth in systems without conservation laws, *Phys. Rev. X* **8**, 021013 (2018).
 - [22] P. Zanardi, Entanglement of quantum evolutions, *Phys. Rev. A* **63**, 040304(R) (2001).
 - [23] G. Styliaris, N. Anand, and P. Zanardi, Information scrambling over bipartitions: Equilibration, entropy production, and typicality, *Phys. Rev. Lett.* **126**, 030601 (2021).

- [24] T. Zhou and D. J. Luitz, Operator entanglement entropy of the time evolution operator in chaotic systems, *Phys. Rev. B* **95**, 094206 (2017).
- [25] S. Pappalardi, A. Russomanno, B. Žunković, F. Iemini, A. Silva, and R. Fazio, Scrambling and entanglement spreading in long-range spin chains, *Phys. Rev. B* **98**, 134303 (2018).
- [26] K. Hashimoto, K.-B. Huh, K.-Y. Kim, and R. Watanabe, Exponential growth of out-of-time-order correlator without chaos: inverted harmonic oscillator, *Journal of High Energy Physics* **2020**, 68 (2020).
- [27] A. W. Harrow, L. Kong, Z.-W. Liu, S. Mehraban, and P. W. Shor, Separation of out-of-time-ordered correlation and entanglement, *PRX Quantum* **2**, 020339 (2021).
- [28] V. Balachandran, G. Benenti, G. Casati, and D. Poletti, From the eigenstate thermalization hypothesis to algebraic relaxation of otocs in systems with conserved quantities, *Phys. Rev. B* **104**, 104306 (2021).
- [29] S. Pilatowsky-Cameo, J. Chávez-Carlos, M. A. Bastarrachea-Magnani, P. Stránský, S. Lerma-Hernández, L. F. Santos, and J. G. Hirsch, Positive quantum lyapunov exponents in experimental systems with a regular classical limit, *Phys. Rev. E* **101**, 010202(R) (2020).
- [30] T. Xu, T. Scaffidi, and X. Cao, Does scrambling equal chaos?, *Phys. Rev. Lett.* **124**, 140602 (2020).
- [31] M. A. Nielsen, A simple formula for the average gate fidelity of a quantum dynamical operation, *Physics Letters A* **303**, 249 (2002).
- [32] C. Murthy and M. Srednicki, Bounds on chaos from the eigenstate thermalization hypothesis, *Phys. Rev. Lett.* **123**, 230606 (2019).
- [33] A. Nahum, J. Ruhman, S. Vijay, and J. Haah, Quantum entanglement growth under random unitary dynamics, *Phys. Rev. X* **7**, 031016 (2017).
- [34] A. Nahum, S. Vijay, and J. Haah, Operator spreading in random unitary circuits, *Physical Review X* **8**, 021014 (2018).
- [35] A. Chan, A. De Luca, and J. T. Chalker, Solution of a minimal model for many-body quantum chaos, *Phys. Rev. X* **8**, 041019 (2018).
- [36] V. Khemani, A. Vishwanath, and D. A. Huse, Operator spreading and the emergence of dissipative hydrodynamics under unitary evolution with conservation laws, *Phys. Rev. X* **8**, 031057 (2018).
- [37] M. P. Fisher, V. Khemani, A. Nahum, and S. Vijay, Random quantum circuits, *Annual Review of Condensed Matter Physics* **14**, 335 (2023).
- [38] Note that the following observation is not valid in some rare cases, where there could be a zero prefactor in front of the leading order on only one side of Eq. (9).
- [39] M. Vanicat, L. Zadnik, and T. Prosen, Integrable trotterization: Local conservation laws and boundary driving, *Phys. Rev. Lett.* **121**, 030606 (2018).
- [40] M. Ljubotina, L. Zadnik, and T. Prosen, Ballistic spin transport in a periodically driven integrable quantum system, *Phys. Rev. Lett.* **122**, 150605 (2019).
- [41] P. W. Claeys and A. Lamacraft, Maximum velocity quantum circuits, *Phys. Rev. Res.* **2**, 033032 (2020).
- [42] T. Zhou and A. W. Harrow, Maximal entanglement velocity implies dual unitarity, *Phys. Rev. B* **106**, L201104 (2022).
- [43] B. Bertini, P. Kos, and T. Prosen, Exact spectral form factor in a minimal model of many-body quantum chaos, *Phys. Rev. Lett.* **121**, 264101 (2018).
- [44] B. Bertini, P. Kos, and T. Prosen, Entanglement spreading in a minimal model of maximal many-body quantum chaos, *Phys. Rev. X* **9**, 021033 (2019).
- [45] B. Bertini and L. Piroli, Scrambling in random unitary circuits: Exact results, *Phys. Rev. B* **102**, 064305 (2020).
- [46] D. A. Roberts and B. Yoshida, Chaos and complexity by design, *J. High Energy Phys.* **2017** (4), 121.
- [47] B. Yan, L. Cincio, and W. H. Zurek, Information scrambling and loschmidt echo, *Phys. Rev. Lett.* **124**, 160603 (2020).
- [48] M. Zonnios, J. Levinsen, M. M. Parish, F. A. Pollock, and K. Modi, Signatures of quantum chaos in an out-of-time-order tensor, *Phys. Rev. Lett.* **128**, 150601 (2022).
- [49] M. M. Wilde, *Quantum Information Theory*, 2nd ed. (Cambridge University Press, 2017).
- [50] G. Chiribella, G. M. D'Ariano, and P. Perinotti, Theoretical framework for quantum networks, *Phys. Rev. A* **80**, 022339 (2009).

Appendix A: Traceless Operators for the OTOC

Here we justify the choice of the operators V and W in the OTOC to be traceless.

Any operator W can be written as sum of a traceless W' and a constant part proportional to the identity, $W = W' + \frac{1}{d_B} \text{tr}[W]$. Using this, the OTOC (2) reduces to

$$\begin{aligned}
 F(W, V_t) &= \text{tr}[W^\dagger V_t^\dagger W V_t] \\
 &= \frac{|\text{tr}[W]|^2}{d_A^2} \text{tr}[\mathbb{1} V_t^\dagger \mathbb{1} V_t] + \frac{\text{tr}[W^\dagger]}{d_A} \text{tr}[\mathbb{1} V_t^\dagger W' V_t] + \frac{\text{tr}[W]}{d_A} \text{tr}[(W')^\dagger V_t^\dagger \mathbb{1} V_t] + \text{tr}[(W')^\dagger V_t^\dagger W' V_t] \\
 &= \text{tr}[(W')^\dagger V_t^\dagger W' V_t] + \text{const},
 \end{aligned} \tag{A1}$$

where we have used the unitary property of V_t and that $\text{tr}[W'] = 0$. Therefore the only non-trivial part of W that leads to OTOC scaling is the traceless unitary W' , and this fact similarly holds for V . Hence wlog we assume W and V to be traceless throughout this work.

2

Appendix C: Proof that maximum entangled Heisenberg operators leads to small OTOC

To derive Eq. (6) algebraically, we start directly from Eq. (5) and use that the Schmidt spectrum of a maximally entangled state is uniform,

$$F(W, V_t) = \sum_{i,j} \frac{1}{d_A^2} \langle \alpha_i | \mathcal{W} | \alpha_i \rangle \langle \beta_j | \beta_j \rangle = \frac{1}{d_A^2} \sum_i \langle \alpha_i | \mathcal{W} | \alpha_i \rangle = \frac{1}{d_A^2} \text{tr}[\mathcal{W}] = \frac{1}{d_A^2} |\text{tr}[W]|^2 = 0. \quad (\text{C1})$$

Here, the final equality is due to imposing the traceless property of W .

Further, choosing the global dynamics to be Haar random, on average one finds that

$$\langle \nu_A \rangle_{U_t \in \mathbb{H}} = \frac{1}{d^2 - 1} (d^2 \rho_\infty - |\phi^+ \rangle \langle \phi^+|) \approx \rho_\infty. \quad (\text{C2})$$

where $\rho_\infty = \mathbb{1}/d$ is the infinite temperature state, and where we have assumed $d \gg 1$ in the final approximation. This can be proven directly, using the expression for the reduced state of $|V_t\rangle$ on $A^{(t)}$ (Eq. (8)),

$$\nu_A(t) := \text{tr}_{\bar{A}^{(t)}}[|V_t\rangle \langle V_t|], \quad (\text{C3})$$

and applying the expression for the 2-fold Haar average, Eq. (D4).

Appendix D: Proof of Theorem 2

Theorem 2. *The averaged OTOC over Haar random, traceless unitaries W (as in Eq. (7)) is equal to*

$$G(V_t) = \frac{1}{d_A^2 - 1} (d_A^2 \langle \phi^+ | \nu_A(t) | \phi^+ \rangle - 1), \quad (9)$$

where $|\phi^+\rangle$ is the maximally entangled state across the doubled system $\mathcal{H}_{S^{(t)}}$.

Proof. Choose the probing unitary W to be Haar random, while preserving its traceless property. That is, consider the average quantity,

$$G := \frac{1}{d} \int dU \text{tr}[U^\dagger W^\dagger U V_t^\dagger U^\dagger W U V_t]. \quad (\text{D1})$$

Recall that each of W , V , and U are local unitary matrices, acting on the spaces A , B and A respectively,

$$W \equiv W_A \otimes \mathbb{1}_{\bar{A}}. \quad (\text{D2})$$

Note also that we take A and B to be disjoint, $B \in \bar{A}$. We write $\tilde{W} \equiv U^\dagger W U \in \mathcal{H}_A$. V_t is in general global for large enough t , so $V_t \in \mathcal{H}_S$. Then

$$\begin{aligned} G &= \frac{1}{d} \int dU \text{tr}[\tilde{W}^\dagger V_t^\dagger \tilde{W} V_t] \\ &= \frac{1}{d} \int dU \text{tr}[(\mathbb{1}_{\bar{A}} \otimes \tilde{W}_A^\dagger) V_t^\dagger (\mathbb{1}_{\bar{A}} \otimes \tilde{W}_A) V_t] \\ &= \frac{1}{d} \int dU \text{tr}[V_t^\dagger (\mathbb{1}_{\bar{A}} \otimes \tilde{W}_A^\dagger) \otimes V_t (\mathbb{1}_{\bar{A}'} \otimes \tilde{W}_{A'}) \mathbb{S}_{SS'}] \\ &= \frac{1}{d} \int dU \text{tr}[(V_t^\dagger \otimes V_t) ((U^\dagger)^{\otimes 2} (W^\dagger \otimes W) (U^{\otimes 2}) \otimes \mathbb{1}_{\bar{A}^{(t)}}) \mathbb{S}], \end{aligned} \quad (\text{D3})$$

where \mathbb{S} is the swap operation. Written in this form in the doubled space, we can see that the Haar average over U is a 2-fold channel of the quantity $W_A^\dagger \otimes W_{A'}$. We can compute this exactly using well-known formula which can be

derived from Weingarten calculus, which states that the 2-fold Haar average (over $U \in \mathcal{H}$, with dimension d) of some tensor $X \in \mathcal{H} \otimes \mathcal{H}$ is [46]

$$\begin{aligned}\Phi_{\text{Haar}}^{(2)}(X) &:= \int dU U \otimes U(X) U^\dagger \otimes U^\dagger \\ &= \frac{1}{d^2 - 1} \left(\mathbb{1} \text{tr}[X] + \mathbb{S} \text{tr}[\mathbb{S}X] - \frac{1}{d} \mathbb{S} \text{tr}[X] - \frac{1}{d} \mathbb{1} \text{tr}[\mathbb{S}X] \right),\end{aligned}\quad (\text{D4})$$

Note also that for any X , by definition the 2-fold Haar average is equal to the 2-fold average over a unitary 2-design, that is $\Phi_{\text{Haar}}^{(2)}(X) = \Phi_{2\text{-design}}^{(2)}(X)$.

Examining the terms of the identity (D4) for $X \equiv W_A^\dagger \otimes W_{A'}$, note that

$$\text{tr}[W_A^\dagger \otimes W_{A'}] = \text{tr}[W_A^\dagger] \text{tr}[W_{A'}] = 0, \text{ and} \quad (\text{D5})$$

$$\text{tr}[W_A^\dagger \otimes W_{A'} \mathbb{S}_{AA'}] = \text{tr}[W_A^\dagger W_A] = \text{tr}[\mathbb{1}_A] = d_A \quad (\text{D6})$$

where the first line is due to the choice of W being traceless, and the second line it due to W being unitary. Therefore in this case only the second and fourth terms in Eq. (D4) are non-zero. Subbing this into Eq. (D3), we arrive at

$$\begin{aligned}G &= \frac{1}{d(d_A^2 - 1)} \text{tr}[(V_t^\dagger \otimes V_t) \left((d_A \mathbb{S}_{AA'} - \mathbb{1}_{AA'}) \otimes \mathbb{1}_{\bar{A}^{(0)}} \right) \mathbb{S}_{SS'}] \\ &= \frac{1}{d(d_A^2 - 1)} \left(d_A \text{tr}[(V_t^\dagger \otimes V_t) \mathbb{1}_{\bar{A}^{(0)}} \mathbb{S}_{\bar{A}\bar{A}'}] - \text{tr}[V_t^\dagger V] \right) \\ &= \frac{1}{d(d_A^2 - 1)} \left(d_A \text{tr}_{\bar{A}^{(0)}}[(\text{tr}_A[V_t^\dagger] \otimes \text{tr}_{A'}[V_t]) \mathbb{S}_{\bar{A}\bar{A}'}] - d \right) \\ &= \frac{1}{d(d_A^2 - 1)} \left(d_A \text{tr}_{\bar{A}}[(\text{tr}_A[V_t^\dagger] \text{tr}_{A'}[V_t])] - d \right)\end{aligned}\quad (\text{D7})$$

Now we notice that

$$\text{tr}_A[V_t] = d_A \langle \phi^+ |_{A^{(0)}} (V_t \otimes \mathbb{1}) | \phi^+ \rangle_{A^{(0)}}. \quad (\text{D8})$$

We have brought out the supernormalization here and in the following, such that $|\phi^+\rangle$ is a normalized quantum state. Subbing this into Eq. (D7), we get

$$\begin{aligned}G &= \frac{1}{d(d_A^2 - 1)} \left(d_A \text{tr}_{\bar{A}}[|d_A \langle \phi^+ |_{A^{(0)}} (V_t \otimes \mathbb{1}) | \phi^+ \rangle_{A^{(0)}}|^2] - d \right) \\ &= \frac{1}{d(d_A^2 - 1)} \left(d_A^3 d_{\bar{A}} \text{tr}_{\bar{A}^{(0)}}[|\langle \phi^+ |_{A^{(0)}} (V_t \otimes \mathbb{1}) | \phi^+ \rangle_{A^{(0)}}|^2 |\phi^+ \rangle_{\bar{A}^{(0)}} \langle \phi^+ |_{\bar{A}^{(0)}}] - d \right)\end{aligned}\quad (\text{D9})$$

Now we recall the definition of the Choi state of the time-evolved local operator V_t , in terms of the maximally mixed state $|\phi^+\rangle$ on the doubled space $\mathcal{H}_S \otimes \mathcal{H}_{S'}$

$$|V_t\rangle := (\mathbb{1}_{S'} \otimes V_t) |\phi^+\rangle. \quad (\text{D10})$$

Then from Eq. (D9)

$$\begin{aligned}G &= \frac{1}{d(d_A^2 - 1)} \left(d_A^3 d_{\bar{A}} \text{tr}_{\bar{A}^{(0)}}[\langle \phi^+ | V_t \rangle \langle V_t | \phi^+ \rangle_{A^{(0)}}] - d \right) \\ &= \frac{1}{d(d_A^2 - 1)} \left(d_A^2 d \text{tr}_{A^{(0)}}[|\phi^+\rangle \langle \phi^+| (\text{tr}_{\bar{A}^{(0)}}[|V_t\rangle \langle V_t|])] - d \right)\end{aligned}\quad (\text{D11})$$

We additionally define the reduced state of $|V_t\rangle$ on $\mathcal{H}_{A^{(0)}}$,

$$\nu_A(t) := \text{tr}_{\bar{A}^{(0)}}[|V_t\rangle \langle V_t|]. \quad (\text{D12})$$

This is a normalized density matrix, and as the reduced state of a pure state it be used can measure the entanglement of this state. Then Eq. (D11) reduces to,

$$G = \frac{1}{d_A^2 - 1} \left(d_A^2 \text{tr}_{A^{(0)}}[|\phi^+\rangle \langle \phi^+| \nu_A(t)] - 1 \right) = \frac{1}{d_A^2 - 1} \left(d_A^2 \mathcal{F}(\nu_A(t), |\phi^+\rangle \langle \phi^+|) - 1 \right) \quad (\text{D13})$$

Where \mathcal{F} is the fidelity of quantum states. \square

Appendix E: Proof of Proposition 3

Proposition 3. *The probability that the OTOC $F(W_R, V_t)$ for some Haar random, traceless unitary W_R varies from the average $G(V_t)$ by more than some $\epsilon > 0$, satisfies*

$$\Pr_{R \sim \mathbb{H}} \{|F(W_R, V_t) - G(V_t)| \geq \epsilon\} \leq \exp\left(-\frac{d_A^2 \epsilon^2}{64}\right). \quad (10)$$

Proof. This proof uses some techniques from that of Proposition 3 from Ref. [23], found in its Supplemental Material. However, we arrive at a smaller Lipschitz constant. We will be applying Levy's Lemma, a concentration of measure result.

Lemma 9. *Levy's Lemma states that for U sampled according to the Haar measure \mathbb{H} , $f : \mathbb{U}_d \rightarrow \mathbb{R}$ a Lipschitz continuous function with Lipschitz constant K , and $\epsilon > 0$ then*

$$\Pr_{U \sim \mathbb{H}} \{|f(U) - \langle f(U) \rangle_{\mathbb{H}}| \geq \epsilon\} \leq \exp\left(-\frac{d\epsilon^2}{4K^2}\right) \quad (E1)$$

where K is defined such that for all $N, M \in \mathbb{U}_d$

$$|f(N) - f(M)| \leq K \|N - M\|_2. \quad (E2)$$

We first need to show that the function

$$f(U) = \frac{1}{d} \text{tr}[U^\dagger W^\dagger U V_t^\dagger U^\dagger W U V_t] \quad (E3)$$

is Lipschitz continuous and determine its constant K . We will use the shorthand notation for superoperators, for $X \in \mathcal{B}(\mathcal{H}_A)$

$$\mathcal{N}(X) := N^\dagger(X)N \otimes \mathbb{1}_{\bar{A}}, \quad (E4)$$

and similarly

$$\mathcal{M}(X) := M^\dagger(X)M \otimes \mathbb{1}_{\bar{A}}. \quad (E5)$$

Then, using Hölder's inequality $|\text{tr}[AB]| \leq \|A\|_\infty \|B\|_1$

$$\begin{aligned} |f(N) - f(M)| &= \frac{1}{d} |\text{tr}[V_t^\dagger (\mathcal{N}(W^\dagger) V_t \mathcal{N}(W) - \mathcal{M}(W^\dagger) V_t \mathcal{M}(W))]| \\ &\leq \frac{1}{d} \|V_t\|_\infty \|\mathcal{N}(W^\dagger) V_t \mathcal{N}(W) - \mathcal{M}(W^\dagger) V_t \mathcal{M}(W)\|_1 \\ &= \frac{1}{d} \|\mathcal{N}(W^\dagger) V_t (\mathcal{N}(W) - \mathcal{M}(W)) - (\mathcal{M}(W^\dagger) - \mathcal{N}(W^\dagger)) V_t \mathcal{M}(W)\|_1 \end{aligned} \quad (E6)$$

Here we have also used that $\|X\|_\infty = 1$ for unitary X , and added and subtracted $\mathcal{N}(W^\dagger) V_t \mathcal{M}(W)$. We can now apply the triangle inequality,

$$\begin{aligned} |f(N) - f(M)| &\leq \frac{1}{d} \left(\|\mathcal{N}(W^\dagger) V_t (\mathcal{N}(W) - \mathcal{M}(W))\|_1 + \|(\mathcal{M}(W^\dagger) - \mathcal{N}(W^\dagger)) V_t \mathcal{M}(W)\|_1 \right) \\ &= \frac{1}{d} \left(\|\mathcal{N}(W) - \mathcal{M}(W)\|_1 + \|\mathcal{M}(W^\dagger) - \mathcal{N}(W^\dagger)\|_1 \right) \end{aligned} \quad (E7)$$

where we have also used that Schatten p norms are unitarily invariant. Then, as $\|X\|_1 \leq \sqrt{d}\|X\|_2$

$$\begin{aligned}
|f(N) - f(M)| &\leq \frac{\sqrt{d}}{d} \left(\|\mathcal{N}(W) - \mathcal{M}(W)\|_2 + \|\mathcal{M}(W^\dagger) - \mathcal{N}(W^\dagger)\|_2 \right) \\
&= \frac{1}{\sqrt{d}} \left(\|\mathcal{N}(W) - \mathcal{M}(W)\|_2 + \|\mathcal{M}(W^\dagger) - \mathcal{N}(W^\dagger)\|_2 \right) \\
&= \frac{2}{\sqrt{d}} \left(\|\mathcal{N}(W) - \mathcal{M}(W)\|_2 \right) \\
&= \frac{2}{\sqrt{d}} \left(\|N^\dagger(W)N - M^\dagger(W)M\|_2 \otimes \mathbb{1}_{\bar{A}} \right) \\
&= \frac{2\sqrt{d_{\bar{A}}}}{\sqrt{d}} \left(\|N^\dagger(W)N - M^\dagger(W)M\|_2 \right)
\end{aligned} \tag{E8}$$

where we have subbed in the definitions (E4) and (E5), and used that $\|X \otimes \mathbb{1}_{\bar{A}}\|_2 = \|X\|_2 \|\mathbb{1}_{\bar{A}}\|_2 = \sqrt{d_{\bar{A}}}\|X\|_2$. We will now apply a similar triangle inequality ‘trick’ as before,

$$\begin{aligned}
|f(N) - f(M)| &\leq \frac{2}{\sqrt{d_A}} \left(\|N^\dagger(W)N - M^\dagger(W)M\|_2 \right) \\
&= \frac{2}{\sqrt{d_A}} \left(\|N^\dagger(W)(N - M) - (M^\dagger - N^\dagger)(W)M\|_2 \right) \\
&\leq \frac{2}{\sqrt{d_A}} \left(\|N^\dagger(W)(N - M)\|_2 + \|(M^\dagger - N^\dagger)(W)M\|_2 \right) \\
&= \frac{4}{\sqrt{d_A}} \|N - M\|_2,
\end{aligned} \tag{E9}$$

where we have again used the unitary invariance of Schatten norms. Therefore, a Lipschitz constant for the OTOC function $f(U)$ is

$$K = \frac{4}{\sqrt{d_A}}. \tag{E10}$$

Directly applying this to Levy’s Lemma completes the proof. \square

Appendix F: Proof of Theorem 4

Theorem 4. (*Scrambling is Necessary for Chaos*) The OTOC, averaged over traceless unitary operators W , is bounded by the entanglement of the time-evolved local operator V_t in the bipartition $(A^{(t)} : \bar{A}^{(t)})$:

A. For geometric measure of entanglement, $E_G(|\phi\rangle) := 1 - \max_{|\psi_{A^{(t)}}\psi_{\bar{A}^{(t)}}\rangle} |\langle \psi_{A^{(t)}}\psi_{\bar{A}^{(t)}} | \phi \rangle|^2$, where the maximum is over all product states $|\psi_{A^{(t)}}\psi_{\bar{A}^{(t)}}\rangle$, $G(V_t)$ satisfies

$$G(V_t) \leq 1 - \frac{d_A^2}{d_A^2 - 1} E_G(|V_t\rangle). \tag{12}$$

B. For the 2-Rényi entropy $S^{(2)}(\nu) := -\log(\text{tr}[\nu^2])$, $G(V_t)$ satisfies

$$G(V_t) \leq \frac{1}{d_A^2 - 1} \left(d_A^2 e^{-\frac{1}{2}S^{(2)}(\nu_{A^{(t)}})} - 1 \right). \tag{13}$$

Proof. **A.** We first define the geometric measure of entanglement for pure states across the bipartition $A : \bar{A}$,

$$E_G(|\phi\rangle) := 1 - \max_{|\psi_A\psi_{\bar{A}}\rangle} |\langle \psi_A\psi_{\bar{A}} | \phi \rangle|^2. \tag{F1}$$

The maximum is taken over all states separable in the splitting $A : \bar{A}$, and $\rho_A := \text{tr}_{\bar{A}}[|\phi\rangle\langle\phi|]$. Then, from Eq. (9), noticing that the first term is equal to the quantum fidelity: $\langle\phi^+|\nu_A(t)|\phi^+\rangle = \mathcal{F}(|\phi^+\rangle\langle\phi^+|, \nu_A(t))$, we have that

$$\begin{aligned}
G(V_t) &= \frac{1}{d_A^2 - 1} \left(d_A^2 \mathcal{F}(|\phi^+\rangle\langle\phi^+|, \nu_A(t)) - 1 \right) \\
&\leq \frac{1}{d_A^2 - 1} \max_{|\psi_A\rangle} \left[d_A^2 \mathcal{F}(|\psi_A\rangle\langle\psi_A|, \nu_A(t)) - 1 \right] \\
&= \frac{1}{d_A^2 - 1} \max_{|\psi_A\rangle} \left[d_A^2 \max_U |\langle\psi_A \psi_{\bar{A}} | \mathbb{1}_A \otimes U_{\bar{A}} | V_t\rangle|^2 - 1 \right] \\
&= \frac{1}{d_A^2 - 1} \max_{|\psi_A\rangle} \left[d_A^2 \max_{|\psi_{\bar{A}}\rangle} |\langle\psi_A \psi_{\bar{A}} | V_t\rangle|^2 - 1 \right] \\
&= \frac{1}{d_A^2 - 1} \left[d_A^2 (1 - E_G(|V_t\rangle)) - 1 \right] \\
&= 1 - \frac{d_A^2}{d_A^2 - 1} E_G(|V_t\rangle)
\end{aligned} \tag{F2}$$

where the third line we have used Uhlmann's Theorem [49].

B. Starting again from Eq. (9), we have that

$$G(V_t) = \frac{1}{d_A^2 - 1} \left(d_A^2 \langle\phi^+|\nu_A(t)|\phi^+\rangle - 1 \right) \tag{F3}$$

Then, we can use the Cauchy-Schwarz inequality for the Hilbert Schmidt inner product, $\langle A, B \rangle_{\text{HS}} := \text{tr}[A^\dagger B]$,

$$\langle\phi^+|\nu_A(t)|\phi^+\rangle = \langle\nu_A(t), |\phi^+\rangle\langle\phi^+|\rangle_{\text{HS}} \leq \sqrt{\text{tr}[\nu_A(t)^2]} \sqrt{\langle\phi^+|\phi^+\rangle^2} = \sqrt{\text{tr}[\nu_A(t)^2]} \tag{F4}$$

to arrive at

$$G(V_t) \leq \frac{1}{d_A^2 - 1} \left(d_A^2 \sqrt{\text{tr}[\nu_A(t)^2]} - 1 \right) \tag{F5}$$

Then,

$$G(V_t) \leq \frac{1}{d_A^2 - 1} \left(d_A^2 e^{-\frac{1}{2} S^{(2)}(\nu_A(t))} - 1 \right), \tag{F6}$$

where the 2-Rényni entropy is defined as $S^{(2)}(\nu) := -\log(\text{tr}[\nu^2])$.

□

Appendix G: Average OTOC vs. LOE for Brickwork Circuits

Here we investigate the scaling of Rényi Entropy $S^{(2)}(\nu_t)$ and the average OTOC $G(V_t)$ in general brickwork circuits, and therefore: (i) show that Eq. (13) is a faithful bound according to the leading order scaling of transfer matrices which we will define (ii) numerically verify that Haar random brickwork circuits show a similar scaling (iii) compute $G(V_t)$ for dual unitary circuits, and show how they compare to known results on LOE from Ref. [16] and (iv) show that Eq. (13) is saturated asymptotically for ‘completely chaotic’ dual unitary circuits. We will use techniques and notation that largely follow Ref. [16]. For further information on the notation used, see therein.

We will use the superoperator (doubled/folder) representation of the components of the local unitary circuit, as in the main text represented with calligraphic script. Graphically, it is convenient to define

$$\mathcal{U} := U \otimes U^* = \text{diagram of a green square with two black lines crossing it} \tag{G1}$$

and its transpose conjugate

$$\mathcal{U}^* := U^\dagger \otimes U^T = \text{diagram of } U^\dagger \otimes U^T \text{ with red box} . \quad (\text{G2})$$

Time runs from top to bottom in these diagrams. Note that each line represents a doubled space. Unitarity then means that

$$\text{tr}_{\text{in}}[U \otimes U^*] = \text{diagram of } U \otimes U^* \text{ with white circles} = \text{diagram of } U \otimes U^* \text{ with red box} = \text{diagram of } U \otimes U^* \text{ with white circles} = \text{diagram of } U \otimes U^* \text{ with white circles}, \quad (\text{G3})$$

and also that

$$(U \otimes U^*)(U^\dagger \otimes U^T) = \text{diagram of } (U \otimes U^*)(U^\dagger \otimes U^T) = \text{diagram of } (U \otimes U^*)(U^\dagger \otimes U^T) = 1. \quad (\text{G4})$$

Here, white circles indicate a projection onto the maximally mixed state on the double space, in other words tracing over the space.

Now consider a local Heisenberg operator V under evolution of a brickwork unitary circuit, the folded diagrammatic representation for its Choi state is

$$|V_t\rangle = \text{diagram of brickwork unitary circuit with } V \text{ at the top} . \quad (\text{G5})$$

Note that every line in this diagram represents a doubled Hilbert space. Here, the black circle represents the Choi state of the local operator,

$$(V \otimes \mathbb{1})|\phi^+\rangle = \text{diagram of } (V \otimes \mathbb{1})|\phi^+\rangle = \text{diagram of } (V \otimes \mathbb{1})|\phi^+\rangle. \quad (\text{G6})$$

Local circuits have a natural ‘lightcone’ from the unitary property of the bricks: applying the graphical rule Eq. (G3), Eq. (G5) reduces to

$$|V_t\rangle = \text{diagram of brickwork unitary circuit with } V \text{ at the top} . \quad (\text{G7})$$

Now, we can use this to come up with a graphical expression for the reduced state of $|V_t\rangle$ on $A^{(t)}$,

$$\nu_A(t) = \text{tr}_{\bar{A}^{(t)}}[|V_t\rangle\langle V_t|] = \text{Diagram} \quad . \quad (\text{G8})$$

Notice that we can further simplify the three top-left gates with the three bottom-left ones using the unitary condition (G4). The resulting expression can then be used to compute the OTOC average $G(V_t)$ (Eq. (9)) and the 2-Rényni entropy $S^{(2)}$, in order to test Eq. (13).

1. Proof of Observation 5

Observation 5. When the term $-\frac{1}{d_A^2-1}$ from Eq. (9) can be neglected, both sides of the inequality Eq. (13) have generically the same leading order scaling for large x_- , but constant x_+ .

Proof. We now define a transfer matrix which yields a convenient description from which to compute quantities in brickwork circuits

$$\mathcal{T}_s[U] = \text{Diagram} \quad . \quad (\text{G9})$$

This transfer matrix appears in both the expression for the 2-Rényni entropy $S^{(2)}(V_t)$ and the OTOC average $G(V_t)$. In particular, for the five layer example in Eq. (G8) ($t = 5/2$, $a = -1/2$, $x_+ = 2$, $x_- = 3$), using the unitarity graphical

identities (G3)-(G4) it is easy to show that

$$G(V_t) = \begin{array}{c} \text{Diagram: A 2x6 grid of diamond-shaped nodes. The first three columns have green diamonds, and the last three columns have red diamonds. Each diamond has four open circles at its corners. The top-left and bottom-right corners of each diamond are connected to the corresponding corners of the diamond to its right. The top-right and bottom-left corners of each diamond are connected to the corresponding corners of the diamond below it. The leftmost and rightmost diamonds have additional connections to external nodes labeled V and V^\dagger respectively. Specifically, the top-left corner of the first green diamond connects to V, and the bottom-right corner of the last red diamond connects to V^\dagger. The top-right and bottom-left corners of the first green diamond and the last red diamond are also connected to external nodes, but these are not explicitly labeled in the diagram. The overall structure represents a tensor network contraction for $G(V_t)$. \end{array} = \langle (\phi^+)^{\otimes 6} | \mathcal{T}_3[U]^2 | V_t \otimes (\phi^+)^{\otimes 4} \otimes V_t^\dagger \rangle. \quad (\text{G10})$$

Whereas, for the 2-Rényni entropy similarly for the example (G8), one can show that

$$e^{-S^{(2)}(\nu_A(t))} = \begin{array}{c} \text{Diagram: A 2x12 grid of diamond-shaped nodes, similar to the one in (G10) but with 12 columns (6 green, 6 red). The top-left and bottom-right corners of each diamond are connected to the corresponding corners of the diamond to its right. The top-right and bottom-left corners of each diamond are connected to the corresponding corners of the diamond below it. The leftmost and rightmost diamonds have additional connections to external nodes labeled V and V^\dagger respectively. The top-right and bottom-left corners of the first green diamond and the last red diamond are also connected to external nodes, but these are not explicitly labeled. The overall structure represents a tensor network contraction for $e^{-S^{(2)}(\nu_A(t))}$. \end{array} = \langle r_6 | \left(\mathcal{T}_3[U]^2 | V_t \otimes (\phi^+)^{\otimes 4} \otimes V_t^\dagger \rangle \right)^{\otimes 2} \quad (\text{G11})$$

where $|r_6\rangle$ ‘rainbow state’ on six sites, i.e. the contraction of indices in the graphical representation of Eq. (G11), formally defined as [16]

$$|r_j\rangle := \frac{1}{d^j} \sum_{I_1, I_2, \dots, I_j}^{d^2} |I_1 I_2 \dots I_j\rangle |I_j I_{j-1} \dots I_1\rangle, \quad (\text{G12})$$

where d refers to the local dimension of a single site here. Recalling that $x_\pm := t \pm a$, in full generality we have that

$$G(V_t) = \langle (\phi^+)^{\otimes 2x_-} | \mathcal{T}_{x_-}[U]^{x_+} | V_t \otimes (\phi^+)^{\otimes (2x_- - 2)} \otimes V_t^\dagger \rangle, \text{ and} \quad (\text{G13})$$

$$e^{-S^{(2)}(\nu_A(t))} = \langle r_{x_-} | \left(\mathcal{T}_{x_-}[U]^{x_+} | V_t \otimes (\phi^+)^{\otimes (2x_- - 2)} \otimes V_t^\dagger \rangle \right)^{\otimes 2}.$$

We note that, in fact, one should define the exponent of \mathcal{T} as $\lceil x_+ \rceil$ and the parameter of \mathcal{T} as $\lfloor x_- \rfloor$, to account for when x_\pm is half integer (this applies also to the results 6-8). One can circumvent this in the main text by just choosing a such that x_\pm is an integer. Then the leading eigenvectors of $\mathcal{T}_{x_-}[U]$ will dominate both the expressions in (G13), for large x_+ , when the term $-\frac{1}{d_A^2 - 1}$ from Eq. (9) can be neglected. Strictly speaking, $\langle (\phi^+)^{\otimes 2x_-} |$ and/or $\langle r_{x_-} |$ could have zero overlap with the leading eigenvector, but this generically won’t happen. Considering λ as the leading non-trivial eigenvalue of $\mathcal{T}_{x_-}[U]$, this means that for a scaling x_+ but constant x_- (i.e. time t and a scaling proportionally), both

$$G(V_t) \sim \lambda^{x_+} \quad (\text{G14})$$

and

$$\sqrt{e^{-S^{(2)}(\nu_A(t))}} \sim \lambda^{x_+}, \quad (\text{G15})$$

Therefore, generically both sides of Eq. (13) have the same asymptotic scaling with large x_+ (large t but constant d_A). \square

2. Random Brickwork Scaling

As a simple test case of Eq. (13), we can choose each brick of a local circuit to be chosen according to the Haar distribution (see details around Theorem 2). In this case we see a similar trend for the left and right hand side of the inequality (13). This is presented in Fig. 3.

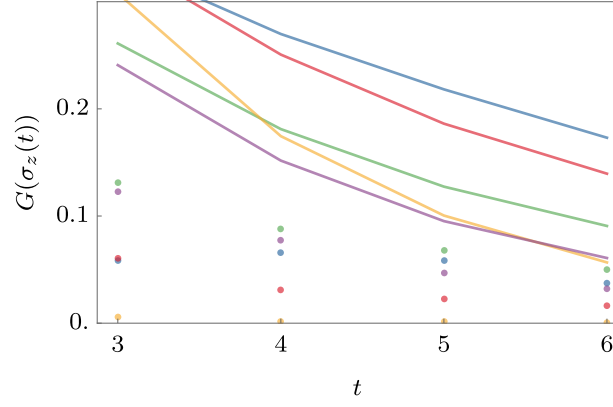


FIG. 3. Comparison of the bound from Eq. (13) (solid lines) and $G(\sigma_z(t))$ (points) for five different evolutions (different colors), which are given by a clean brick-wall quantum circuit made of the same two qubit gate. The five gates were chosen to be Haar random. The bipartition $A^{(t)} : \bar{A}^{(t)}$ is taken to be across half of the total system ($a = 0$).

3. Dual Unitary Circuits (Proof of Theorem 7)

Here we will prove Theorem 7. As explained in the main text, dual unitarity is the extra condition on a brickwork circuit, that each unitary brick is unitary in both *time and space* directions. Graphically, this means that in addition to the graphical rules Eqs. (G3)-(G4), we also have that

$$\text{tr}_{13}[U \otimes U^*] = \text{diagram with green square} = \text{diagram with red square} = \text{diagram with two horizontal lines}, \quad (\text{G16})$$

as well as a spatial analogue of Eq. (G4) (which is not relevant for the present proof, but is relevant for the results we use from Ref. [16]). Using this, we can now prove our main theorem of this section.

Theorem 7. (OTOC in Dual Unitary Circuits) *For evolution according to dual unitary circuits \mathbb{D} , the average OTOC is exactly*

$$G(V_t)|_{\mathbb{D}} = \begin{cases} -\frac{1}{d_A^2-1}, & t \in \ell_A \\ \frac{1}{d_A^2-1} (d_A^2 \langle V | \mathcal{M}_+^{x_+} \mathcal{M}_-^{x_-} | V \rangle - 1), & t \in \ell_{\bar{A}}. \end{cases} \quad (18)$$

Proof. Directly from Eq. (G8) we have that

$$\langle \phi^+ | \nu_A(t) | \phi^+ \rangle = \text{Diagram} \quad (G17)$$

where wlog we have taken V to be local on the site $y = 0$ (as in Fig. 1). We have here first chosen the case where $\mathcal{H}_{\bar{A}^{(t)}}$ is on the left - i.e. that the right light cone of V_t ends up in $\mathcal{H}_{A^{(t)}}$, and so $t \in \ell_A$. In the above diagram, the boundary site between $\mathcal{H}_{A^{(t)}}$ and $\mathcal{H}_{\bar{A}^{(t)}}$ is $a = -1/2$. A direct application of the graphical rules (G3), (G4) and (G16) leads to

$$\langle \phi^+ | \nu_A(t) | \phi^+ \rangle |_{t \in \ell_A} = \begin{array}{c} V^\dagger \text{---} \bullet \text{---} \circ \\ V \text{---} \bullet \text{---} \circ \end{array} = |\text{tr}[V]|^2 = 0, \quad (G18)$$

as V is taken to be traceless. This holds in general when $t \in \ell_A$. If V was instead on site $y = 1$, the condition would change to $t \in \ell_A$ (left light cone in A), and otherwise the results are the same. Therefore wlog we just take $y = 0$ here and in the rest of this work. It can be easily seen that this calculation holds for $y = 0$ and arbitrary a and t , as long as the right lightcone of V_t ends up in $\mathcal{H}_{A^{(t)}}$. Substituting this result into Eq. (9), this completes the proof for the first condition of Eq. (18), when $t \in \ell_A$.

The less trivial, complement situation is when the right light-cone of V ends up in the traced-over region $\bar{A}^{(t)}$,

$-t \in \ell_A$. This corresponds to, for example,

$$\langle \phi^+ | \nu_A(t) | \phi^+ \rangle |_{V \in \mathcal{B}(\mathcal{H}_{\text{even}})} = \text{Diagram}, \quad (\text{G19})$$

where now in this example $a = 1$. Again applying the graphical rules of dual and standard unitarity (Eqs. (G3), (G4) and (G16)), we arrive at the expression

$$\langle \phi^+ | \nu_A(t) | \phi^+ \rangle |_{t \in \ell_{\bar{A}}} = V \bullet \text{Diagram} \bullet V^\dagger, \quad (\text{G20})$$

recalling that $x_\pm := t \pm a$. Graphically, one has that (defined algebraically below Eq. (18))

$$\mathcal{M}_- := \text{Green Diamond} \quad \text{and} \quad \mathcal{M}_+ := \text{Red Diamond}. \quad (\text{G21})$$

Again, this generalizes directly for arbitrary a and t . This therefore completes the proof of Eq. (18) and therefore Theorem 7.

We emphasize that we arrive at this expression only through the assumption of dual unitarity. In particular, no *completely chaotic* assumption from Refs. [16, 41] is needed so far. Further, this expression (G20) is efficient to compute numerically in any dual unitary circuit, with the matrices \mathcal{M}_\pm governing the behavior of two point spatiotemporal correlation functions [9].

Interestingly, we will now see that the completely chaotic property results in an equivalence of chaos and scrambling. To make this explicit, we compare the above results with previous results for LOE. In particular, in Ref. [16] the LOE Rényi entropies for dual unitary circuits in the asymptotic light-cone limits $x_\pm \rightarrow \infty$ are computed. This is achieved for a completely chaotic dual unitary circuit.

The completely chaotic (called ‘maximally chaotic’ in Ref. [41]) property corresponds to the assumption that the eigenvectors with eigenvalue one of transfer matrices $\mathcal{T}_s[U]$ (defined in Eq. (G9)), and an orthogonal transfer matrix (not defined explicitly here, but this is the transfer matrix in the ‘orthogonal lightcone direction’; see Eqs. (37)-(38) in Ref. [16]) are limited to a minimal set. In particular, these minimal eigenvectors can be expressed in terms of the rainbow state (G12), and always trivially have eigenvalue one due to the dual unitary properties. See Eqs. (49)-(51) of Ref. [16] for an explicit definition and derivation. We also note that in Ref. [16], a numerical analysis reveals that the completely chaotic property is highly typical. What this means is that within the set of randomly chosen dual unitary circuits, elements that are not completely chaotic (likely) form a measure zero subset. It would be interesting to prove this claim analytically.

The precise scaling of the 2-Rényni entropy from Ref. [16] directly implies that for general dual unitary circuits,

$$\lim_{x_- \rightarrow \infty} \left(\exp \left[-\frac{1}{2} S^{(2)}(V_t) \right] \right) \geq \langle V_t | \mathcal{M}_+^{x_+} \mathcal{M}_-^{x_-} | V_t \rangle \quad (\text{G22})$$

In particular, Eq. (80) from Ref. [16] is equal to our expression for $\langle \phi^+ | \nu_A(t) | \phi^+ \rangle$ in Eq. (18) (note that our expressions for x_{\pm} in this paper are reversed compared to [16], due to labeling conventions). Then for $G(V_t)$ in the limit $x_- \rightarrow \infty$, the multiplicative factor and additive constant go to one and zero respectively, as $d_A \rightarrow \infty$. The equality holds under the completely chaotic assumption and for $|\lambda| \geq d^{-1/2}$, with the consecutive limits $x_+ \rightarrow \infty$ and $x_- \rightarrow \infty$ (as also necessarily $d_A \rightarrow \infty$). Here $|\lambda|$ is the largest non-trivial eigenvalue of \mathcal{M}_- . The more general Eq. (G22) also follows directly from Ref. [16], where we notice that the expression for purity can contain additional positive terms for non completely chaotic examples, and in finite time, resulting in an inequality.

We therefore arrive at Eq. (19) and therefore concluding the proof of Theorem 8. □

Appendix H: Proof of Theorem 6

Theorem 6. (*Scrambling without Chaos*) *The Floquet dual-unitary XXZ model (16) produces an exponentially decaying OTOC. Concretely, for a single site operator V , Eq. (18) reduces to*

$$G(V_t)|_{\text{XXZ}} = \begin{cases} \frac{-1}{d_A^2 - 1}, & \text{if } t \in \ell_A \\ \beta e^{-\alpha(x_-)} + (1 - \beta), & \text{if } t \in \ell_{\bar{A}}. \end{cases} \quad (\text{17})$$

with positive constants α and β reported in Eq. (H6). For any V orthogonal to σ_z , the constants are such that $G(V_t)$ decays to a minimal (negative) value.

Proof. Expanding the single-site unitary qubit operator V in the Pauli basis, we have that

$$\begin{aligned} V &= a_1 \mathbb{1} + a_x \sigma_X + a_y \sigma_Y + a_z \sigma_Z \\ &= a_x \sigma_X + a_y \sigma_Y + a_z \sigma_Z \end{aligned} \quad (\text{H1})$$

as $\text{tr}[V] = 0 \iff a_1 = 0$. As we consider the normalized Choi state $|V\rangle$, we also have that

$$a_z^2 = 1 - (a_x^2 + a_y^2). \quad (\text{H2})$$

From Theorem 7 we know that in dual unitary circuits,

$$G(V_t) = \frac{1}{d_A^2 - 1} \left(d_A^2 \langle V | \mathcal{M}_+^{x_+} \mathcal{M}_-^{x_-} | V \rangle - 1 \right). \quad (\text{H3})$$

Now, using the full classification of dual unitary circuits for qubits [9], we know that \mathcal{M}_{\pm} for the XXZ model for qubits takes the simple form in the Pauli basis

$$\mathcal{M}_{\pm} = \text{diag}(1, \sin(2J), \sin(2J), 1). \quad (\text{H4})$$

Substituting Eqs. (H1) and (H4) into Eq. (H3), evaluating in the Pauli basis

$$\begin{aligned} G(V_t)_{\text{XXZ}} &= \frac{1}{d_A^2 - 1} \left(d_A^2 ((a_x^2 + a_y^2) \sin(2J)^{2(x_-)} + a_z^2) - 1 \right) \\ &= \frac{1}{d_A^2 - 1} \left(d_A^2 ((a_x^2 + a_y^2) \sin(2J)^{2(x_-)} - (a_x^2 + a_y^2)) \right) + 1, \end{aligned} \quad (\text{H5})$$

where we have used Eq. (H2). This corresponds to the exponential behavior decay with (x_-) , as $\sin(2J) < 1$ given that $J \neq \pi/4$. For clarity of notation, we arrive at Eq. (17) by setting

$$\begin{aligned} \alpha &= \ln\left(\frac{1}{\sin(2J)}\right), \text{ and} \\ \beta &= d_A^2 (a_x^2 + a_y^2) / (d_A^2 - 1). \end{aligned} \quad (\text{H6})$$

From this, for $a_z = 0$ and taking the limit $(x_-) \rightarrow \infty$ we arrive at

$$\lim_{(x_-) \rightarrow \infty} (G(V_t)_{\text{XXZ}}|_{a_z=1}) = \frac{-1}{d_A^2 - 1}. \quad (\text{H7})$$

□

Appendix I: Operator Free Generalization

Here we argue that a operator-free generalization of the OTOC and of the LOE are related in a straightforward manner, generalizing the main results of the Letter. These CP operators encode all possible OTOCs and local Heisenberg operator Choi states (from which to compute the LOE), analogous to defining a density matrix in quantum mechanics to encode all possible measurements which one could make. One can probe novel properties of this CP operator generalization, such as the conditional mutual information which allows one to distinguish between genuine quantum scrambling and decoherence (as in Ref. [48]).

The ‘out-of-time-order tensor’ (OTOT) is defined as the CP operator $\Upsilon^{\text{OTOT}} \in \mathcal{H}_{B_i} \otimes \mathcal{H}_A \otimes \mathcal{H}_{B_f}$ such that [48]

$$F(W, V_t) = \text{tr}[\Upsilon^{\text{OTOT}}(\mathcal{V} \otimes \mathcal{W} \otimes \mathcal{V}^*)]. \quad (\text{I1})$$

Full definitions and further details can be found in Ref. [48]. The space $B_{i/f}$ are the same spatial Hilbert spaces at the start and end of the OTOC protocol, which are technically independent spaces in the quantum combs formalism. We further take the initial state in the OTOT definition to be maximally mixed $\rho \sim \mathbb{1}$. Then for a choice of the operations \mathcal{V} and \mathcal{W} , one gets exactly the usual OTOC $F(W, V_t)$ from the tensor Υ^{OTOT} .

Similarly, we can generalize the LOE to a ‘local tensor entanglement’ (LTE), for the CP operator $\Upsilon^{\text{LTE}} \in \mathcal{H}_{B'} \otimes \mathcal{H}_S$ [19],

$$\Upsilon^{\text{LTE}} := \mathcal{U}_S \left(\frac{\mathbb{1}_{\bar{B}}}{d_{\bar{B}}} \otimes |\phi^+\rangle \langle \phi^+|_{B^{(v)}} \right). \quad (\text{I2})$$

As detailed in Ref. [19], if one projects with some choice of maximally entangled state onto the ancilla B' , one gets exactly the time evolved Heisenberg operator. From this, the usual LOE can be computed. For example, for a qubit space \mathcal{H}_B , projecting onto the ancilla space $\mathcal{H}_{B'}$ with the ψ^+ bell state results in,

$$\langle \psi^+ | \Upsilon^{\text{LTE}} | \psi^+ \rangle = \Upsilon_{S|x} = X_t, \quad (\text{I3})$$

where X_t is the time evolved Pauli-X operator.

Our results from the main body can easily be framed in terms of these two objects.

Observation 10. *The LTE and OTOT are related via*

$$\Upsilon_{B_i A_t B_f} = \text{tr}_A [\Upsilon_{N_i S_t} * \Upsilon_{N_f S_t}^*] \quad (\text{I4})$$

where the right hand side is the link product, giving a Hilbert Schmidt inner product on the complement to the probe space, $\mathcal{H}_{\bar{A}}$, and a tensor product on \mathcal{H}_A [50] (see below in Eq. (I5)). Note that $B_{i/f} \equiv N_{i/f}$ due to projection with the maximally entangled state in the definition Eq. (I2).

This observation is immediately apparent graphically, in that

$$\Upsilon^{\text{OTOT}} = \text{Diagram} \quad (\text{I5})$$

From this, all previous results will directly generalize to this operator-free setting. This is revealing of the close connection between the OTOC and LOE [19].